Optimum Graft Density for Dispersing Particles in Polymer Melts

Ryuichi Hasegawa,†,‡ Yuji Aoki,† and Masao Doi*,‡

Yokkaichi Research Center, Mitsubishi Chemical Co., Toho-cho, Yokkaichi, Mie 510, Japan, and Department of Applied Physics, Nagoya University, Chikusa-ku, Nagoya, Aichi 464, Japan

Received March 1, 1996; Revised Manuscript Received June 17, 1996[⊗]

ABSTRACT: We investigate the dispersion of polymer-grafted particles suspended in a polymer matrix by viscoelastic measurements and electron microscopy. We find that, when the graft density is low, the particle dispersion improves with an increase of the graft density, while the particle dispersion becomes worse when the graft density is too high; i.e., there is an optimum graft density for dispersing the particles. We explain the phenomena by showing that the grafted polymers cause attraction for high graft density.

1. Introduction

Rheological properties of particle suspensions are strongly dependent on the surface forces acting between the particles. If the force is purely repulsive, the suspension is a fluid with low viscosity. However, if the force has an attractive part, the suspension becomes a very viscous liquid or a gel.

Various techniques have been used to control the surface forces.[1,2] One way to enhance the repulsive forces is to graft polymers on the surface of the particles. This technique works if the suspending medium is a good solvent for the polymer. However, the effect of the grafted polymer is delicate if the suspending medium contains polymers.[3] Gast and Leibler[4] calculated the surface forces between the polymer-grafted layer in polymer solutions and found that increasing the graft density can cause flocculation of particles in polymer solutions. This effect has been attributed to the depletion effect.[1,2]

In this paper, we consider the same problem for polymer melts: does increasing the graft density enhance the repulsion between the polymer-grafted particles if the suspending medium is a polymer melt? This work was motivated by experiments on ABS polymers conducted by one of us.[5] ABS polymers consist of poly(acrylonitrile-*co*-styrene) (AS) grafted on polybutadiene (PB) particles dispersed in linear AS. PB particles are cross-linked thermally, and they behave as hard spheres in the AS melt. It was found that grafting AS polymers on the particles enhances the particle dispersions if the graft density is low, but it causes flocculation if the graft density becomes too high. In this paper, we will calculate the interaction force between the polymer-grafted surfaces in polymer melts by a mean field approximation and show that the force can have an attractive part if the graft density is too high. This explains the above experimental results.

The finding that the interaction becomes attractive if the graft density is too high is qualitatively consistent with the prediction of Gast and Leibler[4] for polymer solutions, but the details of the attractive force are not the same. In particular, the attractive force in polymer melts depends on the length of the grafted polymers, while it is independent of the length of the grafted polymers in polymer solutions. The attractive force that we observed is rather similar to the case of diblock copolymer/homopolymer blends.[16−18]

2. Experimental Section

2.1. Materials. ABS polymers were synthesized by emulsion polymerization.[5] Table 1 shows the characteristics of ABS polymers used in the present work. The diameter D of the PB particles has a very narrow distribution[6] ($D_w/D_n < 1.01$). The grafting degree g_d is the ratio between the weight of the grafted polymers W_g and the weight of PB particles W_p; g_d can be determined from the acetone-insoluble part of the ABS polymers. Given g_d, the graft density σ, which is the number of polymers per unit surface area of the particle, can be calculated as follows. Let n be the number of particles per unit volume, then W_g is written as

$$W_g = 4\pi(D/2)^2\sigma(M_g/N_A)n \tag{1}$$

where M_g is the molecular weight of the grafted polymer and N_A is Avogadro's number. On the other hand, the weight of the particles W_p per unit volume is given by

$$W_p = (4\pi/3)(D/2)^3\rho_p n \tag{2}$$

where ρ_p is the density of the particle. From eqs 1 and 2, it follows that σ is calculated from the grafting degree $g_d = W_g/W_p$ as

$$\sigma = g_d D\rho_p N_A/6M_g \tag{3}$$

Notice that σ of our end-grafted polymers is much higher than that of adsorbed polymers.

The grafted polymers and the matrix polymers are both random copolymers, and, in general, their compositions are not equal to each other. However, the composition difference between the two in our samples was very small. This was checked as follows. After ozonolysis of the acetone-insoluble part of the ABS polymers, acrylonitrile content, AN%, and the molecular weight of grafted AS copolymers were measured: AN% is measured by elementary analysis (Yanaco, CHN corder), and the weight-average molecular weight (M_w) and the polydispersity index (M_w/M_n) are determined by GPC (Waters, 150C ALC/GPC) in tetrahydrofuran. The analysis indicated that the AN% difference between the grafted polymer and matrix polymer is very small and that the molecular weight of the graft chain is almost the same as or slightly larger than that of the matrix polymer.

To change the PB content in the ABS sample, the original ABS polymers were blended with AS copolymer. Blending was performed at 200 °C for 10 min by using a Brabender Plasticoder.

* To whom correspondence should be addressed. Phone: 81-52-789-3718. FAX: 81-52-789-3719.
† Mitsubishi Chemical Co.
‡ Nagoya University.
⊗ Abstract published in *Advance ACS Abstracts,* August 15, 1996.

S0024-9297(96)00365-8 CCC: $12.00

Table 1. Molecular Characteristics of the ABS Polymers Used in the Present Experiments

	Graft									
particle diameter D (nm)	350	350	350	350	350	350	170	170	170	170
grafting degree, g_d	0.165	0.177	0.264	0.344	0.367	0.586	0.232	0.413	0.687	1.109
$M_w/10^3$ (g/mol)	93	90	88	84	70	84	75	88	100	109
graft density, σ (nm^{-2})	0.062	0.069	0.105	0.143	0.185	0.244	0.053	0.080	0.117	0.173
	Matrix									
$M_w/10^3$ (g/mol)	58	58	58	58	58	58	58	58	58	58

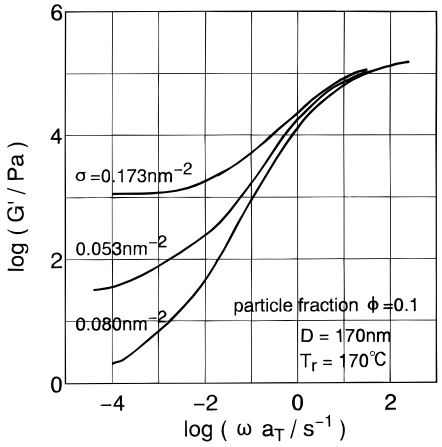

Figure 1. Master curves of the storage shear modulus G' for ABS polymers at 170 °C: PB particle fraction, 0.1; PB particle diameter, 170 nm.

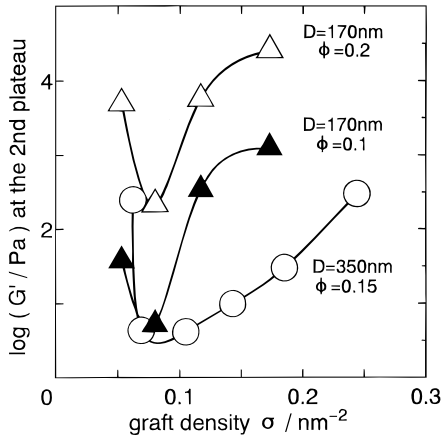

Figure 2. Storage shear modulus G' at $\omega a_T = 10^{-3}$ s^{-1} of ABS polymers plotted against graft density σ.

2.2. Dynamic Viscoelastic Measurement. A concentric cylinder-type rheometer was used for measurements of dynamic viscoelastic properties of the samples. The measurements were done by varying the temperature from 155 to 230 °C and the frequency from 6.67×10^{-4} to 1.0 Hz. Measurements were performed under nitrogen so as to minimize the oxidative degradation at high temperature. The time−temperature superposition principle was used to obtain the master curves.

Figure 1 shows the master curves for the storage shear modulus. Here, the reference temperature is 170 °C. It is seen that G' shows a plateau in the low-frequency region. The plateau, called the second plateau, arises from the interaction between the particles and is strongly correlated with the state of particle dispersions: the worse the dispersion (i.e., the stronger the particle attraction), the higher the second plateau. It has seen that, as the graft density σ increases, the height of the second plateau first decreases and then increases again. This indicates that there is an optimum graft density to disperse PB particles.

To find the optimum graft density, we plotted the value of G' at $\omega a_T = 10^{-3}$ s^{-1} as a function of the graft density σ in Figure 2. The second plateau has a minimum at a characteristic graft density σ_c, which we call the optimum graft density.

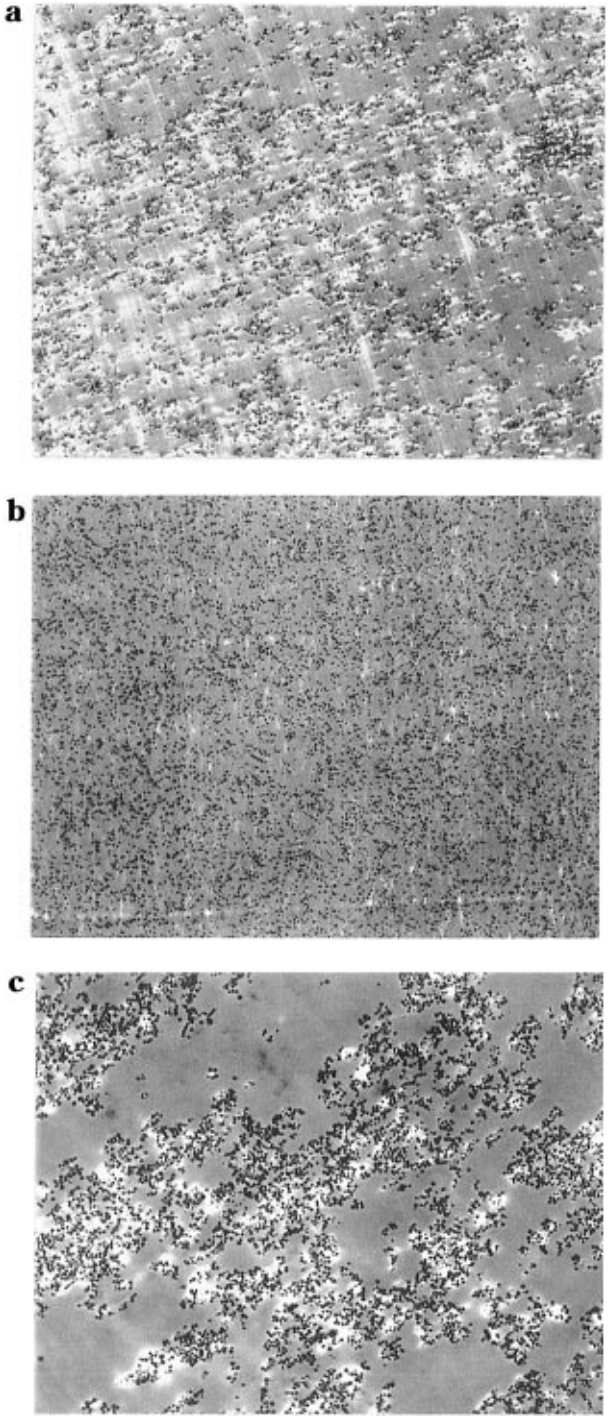

Figure 3. Electron micrographs of ABS polymers. They are taken after dynamic viscoelastic measurement. PB particle fraction, 0.1; PB particle diameter, 170 nm. (a) $\sigma = 0.053$ nm^{-2}, (b) $\sigma = 0.080$ nm^{-2}, (c) $\sigma = 0.173$ nm^{-2}.

It is important to note that the optimum graft density σ_c is independent of particle content and particle size. This suggests that σ_c is determined essentially by the surface force between the particles.

2.3. Electron Microscopic Observation. To confirm that the minimum of the second plateau corresponds to the

best dispersion, we conducted transmission electron microscopic (TEM) observations after measurement of the dynamic viscoelasticity. According to the method developed by Kato,[20] ultrathin sections were prepared after PB particles were stained by osmium tetraoxide. Figure 3 gives the TEM micrographs of three samples whose graft densities are below σ_c, near σ_c, and above σ_c, respectively. The sample near σ_c is clearly the best dispersed among the three. This confirms that σ_c corresponds to the state of the least attractive force.

3. Theoretical Section

3.1. Mean Field Calculation. To understand the above phenomena, we calculate the interaction free energy between the particles. For this purpose, we first consider two polymer-grafted plates placed parallel to each other in an polymer melt and study how the free energy changes when the separation between the two plates H is changed. We take the z-axis normal to the plates and place each plate at $z = 0$ and $z = H$. We assume that the grafted polymers and the matrix polymers (or the free polymers) are made of the same monomers, having degrees of polymerization N_g and N_f, respectively. This assumption disregards some of the complexity in the real system: in our ABS system, both the grafted polymer and the matrix polymers are random copolymers,[7] and there is molecular weight distribution. In this paper, however, we postpone the study of these effects to future works and concentrate here on the simplest case.

To calculate the interaction energy, we use mean field theory. This generally reduces to solving a Schrödinger-type equation for the wave function $\Psi(z,n)$, which represents the statistical weight of polymer segment n located at position z in a mean field potential $V(z)$:

$$\frac{\partial \Psi}{\partial n} = \frac{a^2}{6}\left(\frac{\partial^2 \Psi}{\partial z^2}\right) - V\Psi \tag{4}$$

In the present problem, there are three kinds of polymers: the matrix polymer (the free polymer), the polymers grafted on the first plate at $z = 0$, and the polymers grafted on the second plate at $z = H$. We use the suffixes f, g_1, and g_2 to distinguish these and introduce three functions: $\Psi_f(z,n)$, $\Psi_{g_1}(z,n)$, and $\Psi_{g_2}(z,n)$. In the actual calculation, we use the formulation of Scheutjens and Fleer et al.[8] In this formulation, the polymer is represented by a walk on a lattice, and the Schrödinger-type eq 4 is represented by the following recurrence relation:

$$\Psi_\alpha(z,n+1) = \exp[-V(z)][(^1/_6)\Psi_\alpha(z-a,n) + (^4/_6)\Psi_\alpha(z,n) + (^1/_6)\Psi_\alpha(z+a,n)] \qquad \text{for } \alpha = \text{f, } g_1, g_2 \tag{5}$$

The boundary conditions at $z = 0$ and $z = H$ are

$$\Psi_\alpha(0,n) = \Psi_\alpha(H+a,n) = 0 \qquad \text{for } \alpha = \text{f, } g_1, g_2 \tag{6}$$

The initial conditions respectively are given by

$$\Psi_f(z,1) = \exp[-V(z)] \tag{7}$$

$$\Psi_{g_1}(z,1) = \begin{cases} \exp[-V(z)] & \text{for } z = a \\ 0 & \text{otherwise} \end{cases} \tag{8}$$

$$\Psi_{g_2}(z,1) = \begin{cases} \exp[-V(z)] & \text{for } z = H \\ 0 & \text{otherwise} \end{cases} \tag{9}$$

The segment densities $\Phi_i(z)$ for each component are calculated with the composition law:

$$\Phi_f(z) = \sum_{n=1}^{N_f} \frac{\Phi_f^{bulk}}{N_f} \exp[V(z)]\, \Psi_f(z,n)\, \Psi_f(z, N_f - n + 1) \tag{10}$$

$$\Phi_{g_i}(z) = \sum_{n=1}^{N_g} \frac{\sigma}{\sum_z \Psi_{g_i}(z,N_g)} \exp[V(z)]\Psi_{g_i}(z,n)\Psi_f(z,N_g - n + 1) \tag{11}$$

where Φ_f^{bulk} is the concentration of free polymer in the bulk and is taken to be unity. The self-consistent potential $V(z)$ is determined by the incompressible condition:

$$\Phi_f(z) + \Phi_{g_1}(z) + \Phi_{g_2}(z) = 1 \qquad \text{at any } z \tag{12}$$

The above equations are solved self-consistently. To avoid the computational underflow that arises for high graft density and large N_g and N_f, we used the rescaling procedure proposed by Wijmans et al.[9] Once the self-consistent solution is obtained, the excess surface free energy F_s of the system per unit area of the plate is calculated as[10]

$$F_s(H) = F_{sg}(H) + F_{sf}(H) \tag{13}$$

where $F_{sg}(H)$ and $F_{sf}(H)$ represent the contributions of the grafted polymer and the matrix polymer, respectively. They are written as

$$F_{sg}(H)/a^{-2}kT = \sum_{i=1,2}[\sigma \ln(\sigma N_g(\sum_{z=a}^{H}\Psi_{g_i}(z,N_g))^{-1}) - \sum_{z=a}^{H} V(z)\Phi_{g_i}(z)] \tag{14}$$

$$F_{sf}(H)/a^{-2}kT = \sum_{z=a}^{H}\frac{\Phi_f(z)}{N_f}\ln \Phi_f^{bulk} - \sum_{z=a}^{H} V(z)\Phi_f(z) = -\sum_{z=a}^{H} V(z)\Phi_f(z) \tag{15}$$

where we have used $\Phi_f^{bulk} = 1$. The interaction free energy at separation H is

$$F_{pol}(H) = F_s(H) - F_s(\infty) \tag{16}$$

where $F_s(\infty)$ is the excess surface free energy at infinite separation. The interaction energy between two spherical particles with diameter D separated by distance H can be calculated by using the Derjagin approximation:[21]

$$A_{pol}(H) = \pi D \int_H^\infty F_{pol}(z)\, dz \tag{17}$$

3.2 Results. Figure 4 shows the interaction free energy $F_{pol}(H)$ as a function of the particle separation H for various graft densities σ. When the graft density is low, $F_{pol}(H)$ has repulsive part only. The origin of the repulsion is essentially the excluded volume effect between the grafted polymer. As the graft density increases, the grafted polymer is more stretched. Accordingly, the interaction range of the repulsive part increases. However a striking fact is that there also appears an attractive part at the end of the repulsive part. In the next section, we shall discuss the origin of

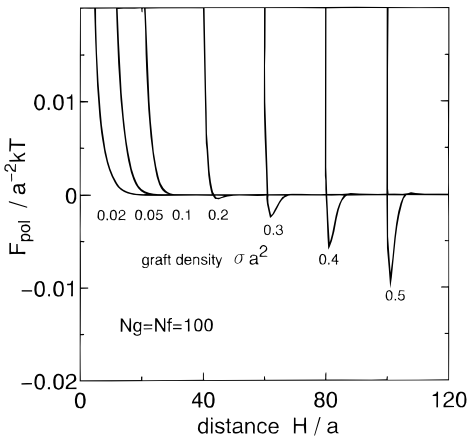

Figure 4. Interaction free energy per unit area F_{pol} between two brushes ($N_g = 100$) placed in polymer melt ($N_f = 100$), plotted against the distance H for various graft densities $\sigma a^2 = 0.02 - 0.5$.

the attractive part. Here we identify the appearance of the attractive part as the origin of the existence of the optimum graft density.

In real systems, there is a van der Waals attraction between the particles:[2]

$$A_{vdw}(H) = -\frac{AD}{12H} \qquad \text{(A is the Hamaker constant)} \tag{18}$$

The actual interaction $A_{int}(H)$ is the sum of $A_{pol}(H)$ and $A_{vdw}(H)$:

$$A_{int}(H) = A_{pol}(H) + A_{vdw}(H) \tag{19}$$

Since the van der Waals part $A_{vdw}(H)$ has a negative value which depends weakly on H, the total interaction energy $A_{int}(H)$ has the following characteristics. When the graft density is low, $A_{pol}(H)$ is a hard-core-like repulsion, so $A_{int}(H)$ assumes a minimum at the end of the repulsive core. As the graft density increases, the thickness of $A_{pol}(H)$ increases. This decreases the depth of the minimum of the total interaction energy $A_{int}(H)$. Thus, at low graft density, the maximum attraction decreases with an increase of the graft density. This gives better dispersion of particles.

On the other hand, if the graft density becomes very large, there appears an attractive part in $A_{pol}(H)$, and its depth increases with increasing graft density. Therefore, the dispersion becomes worse if the graft density becomes too high. This is the origin of the optimum graft density.

To demonstrate the above qualitative explanation, we calculated the particle−particle interaction potential $A_{int}(H)$ for particular cases and show the results in Figure 5. Here, the parameters are as follows: the degree of polymerization of grafted and matrix polymers $N_g = N_f = 100$, the segment size $a = 1$ nm, Hamaker constant $A = 10^{-20}$ J,[2] particle diameters $D = 200$ and 400 nm, and the graft density is shown in the figure. In all cases, $A_{int}(H)$ has an attractive part, and the minimum of the attractive part varies with the graft density. The optimum graft density corresponds to the σ that gives the least depth of the attraction. This corresponds to $\sigma = 0.1$ nm^{-2}, which compares well with the optimum graft density shown in Figure 2. Also notice that the optimum graft density is independent of the particle diameter.

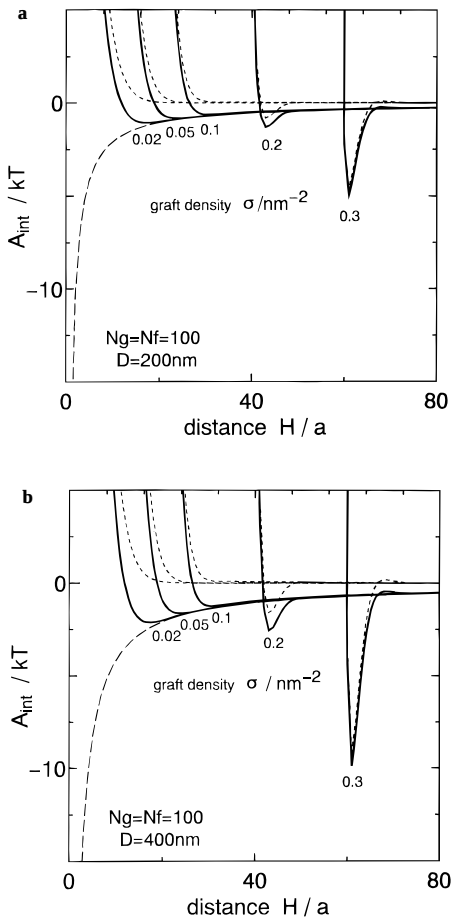

Figure 5. Particle−particle interaction energy $A_{int}(H) = A_{pol} + A_{vdw}$, plotted against the separation H between particles for $N_g = N_f = 100$ and various σ. Solid lines are A_{int}, dashed lines A_{pol}, and broken lines A_{vdw}. (a) $D = 200$ nm; (b) $D = 400$ nm. In both cases, the depth of the attraction energy becomes minimum at $\sigma = 0.1$ nm^{-2}.

3.3 Origin of the Attractive Potential. Having seen that the existence of the optimum graft density corresponds to the appearance of the attractive part in $F_{pol}(H)$, we now consider the origin of the attractive part.

In the follow, we shall consider the case of $N_f \gtrsim N_g$. In this case, it has been shown[12] that the grafted polymer is highly stretched if $\sigma a^2 \gtrsim N_g^{-1/2}$ (the brush regime), while the grafted polymer is in a randomly coiled conformation if $\sigma a^2 \lesssim N_g^{-1/2}$ (the mushroom regime). Since the attraction is observed for high graft density, we first consider the case of the brush regime.

Now we show that the attractive potential arises mainly from the matrix term $F_{sf}(H)$ rather than the graft term $F_{sg}(H)$. This is because the polymer conformation in the matrix is strongly affected as the particles come close to each other, while the polymer conformation in the brush is less affected. To demonstrate this, we plot $F_{sf}(H)$ and $F_{sg}(H)$ against H in Figure 6. It is seen that the attractive potential is given mainly by the matrix term $F_{sf}(H)$; the brush term changes little with H. Thus, we may approximate $F_{pol}(H)$ as

$$F_{pol}(H) = F_{sg}(H) - F_{sg}(\infty) + F_{sf}(H) - F_{sf}(\infty)$$
$$\simeq F_{sf}(H) - F_{sf}(\infty) \tag{20}$$

It must be noted that this approximation is good for high graft density; when the graft density is low, the confor-

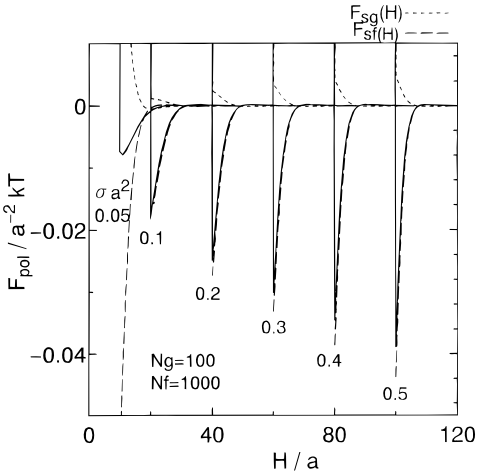

Figure 6. Interaction free energy $F_{pol}(H)$ between parallel brushes and its two components $F_{sg}(H)$ and $F_{sf}(H)$, plotted against H. The attraction is caused by the matrix term $F_{sf}(H)$.

mation of the grafted polymer changes significantly with H, and eq 20 is not valid. We shall return to this point later.

Now, to estimate $F_{sf}(H)$ using eq 15, we examine the behavior of the integrand $V(z)\Phi_f(z)$. First, we consider the case that the plates are placed far apart. In this case, there is no interaction between the plates, and the problem is to consider one graft layer, placed in a polymer matrix. This problem has been studied by several groups,[11−13] and it has been shown[12] that the matrix polymer and the grafted polymer barely mix with each other; the grafted polymer forms a dense layer of thickness

$$L = N_g \sigma a^3 \tag{21}$$

which is determined by the volume filling condition. Figure 7a shows the segment distribution of the grafted polymer $\Phi_g(z)$ calculated by mean field theory. The segment density is equal to 1 in the brush region and falls sharply to zero at the interface. The profile can be fitted by

$$\Phi_g(z) = (^1/_2)\left(1 - \tanh\frac{z - L}{\lambda}\right) \tag{22}$$

where λ is the penetration depth of the matrix polymer into the brush region. Leibler and Ajdari[13] have shown that λ is given by

$$\lambda \simeq a\left(\frac{N_g}{\sigma a^2}\right)^{1/3} \tag{23}$$

We have checked numerically that the relation $\lambda \propto N_g^{1/3}\sigma^{-1/3}$ indeed holds for the cases shown in Figure 7.

Figure 7 shows the segment potential $V(z)$. If the graft density is not too low (if $\sigma a^2 \gtrsim 0.2$), the segment potential $V(z)$ is almost parabolic. The parabolic part can be understood by the classical approximation,[14] according to which

$$V_{cl}(z) = \frac{\pi^2}{24 N_g^2}\left[(N_g \sigma a^2)^2 - \left(\frac{z}{a}\right)^2\right] \tag{24}$$

However, there is a small deviation from this form at the edge of the brush region, i.e., $z \simeq L$. The potential $V(z)$ becomes negative for $z > L$. This dip in $V(z)$ can

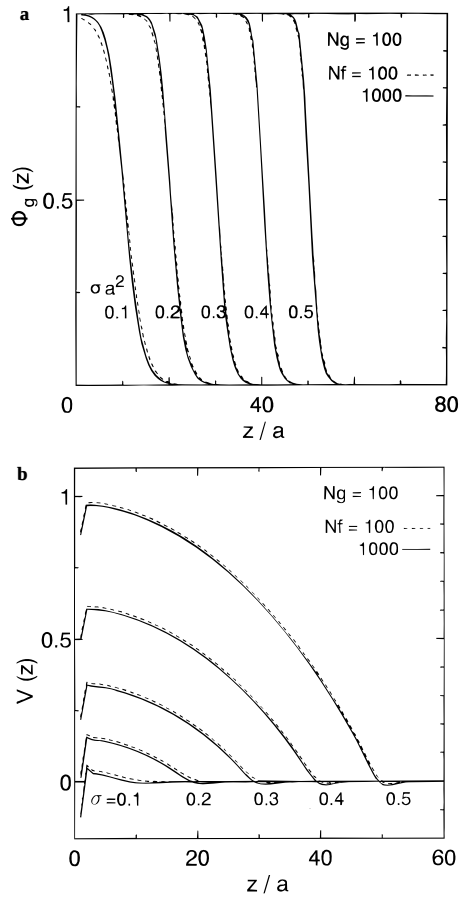

Figure 7. Segment density $\Phi_g(z)$ (a) and segment potential $V(z)$ (b) of single brush ($N_g = 100$) in polymer matrix ($N_f = 100$, 1000) for various graft densities σ (solid lines, $N_f = 1000$; dashed lines, $N_f = 100$).

be understood as follows. Let us consider the case of $N_f \gg N_g$; then, we can use the ground state approximation (GSA) for the matrix polymer. This approximation is written, in the continuum limit, as

$$\frac{a^2}{6}\left(\frac{d^2\Psi_f}{dz^2}\right) - V\Psi_f = 0 \tag{25}$$

and the composition law eq 10 reduces to

$$\Phi_f = \Psi_f^2 = 1 - \Phi_g(z) \tag{26}$$

If we substitute the hyperbolic tangent density profile $\Phi_f(z) = (^1/_2)(1 + \tanh[(z - L)/\lambda)]$ into the above equations, we obtain

$$V_{GSA}(z) = \frac{\exp\left(-\frac{2(z-L)}{\lambda}\right) - 2}{6\lambda^2\left(\exp\left(\frac{z-L}{\lambda}\right) + \exp\left(-\frac{z-L}{\lambda}\right)\right)^2} \tag{27}$$

In Figure 8, eq 27 is compared with the results of the full mean field calculation. Here we plot $V(z)\Phi_f(z)$ rather than $V(z)$ itself, since GSA is valid only outside the brush region. It is seen that the results of the mean field calculation agree with GSA reasonably well. Thus, in the following, we use the approximation

$$V(z)\Phi_f(z) \approx V_{GSA}(z)\Phi_f(z) = \frac{a^2}{6}\frac{d^2\Psi_f}{dz^2}\Psi_f \tag{28}$$

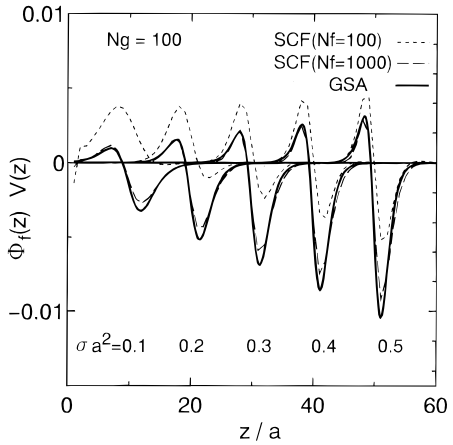

Figure 8. Comparison between the full mean field calculation and GSA calculation for the potential $V(z)$.

Using eqs 15 and 28, the interaction free energy is now given by

$$F_{sf}(\infty)/a^{-2}kT = -2\frac{a^2}{6}\int_0^\infty dz \frac{d^2\Psi_f}{dz^2}\Psi_f = 2\frac{a^2}{6}\int_0^\infty dz \left(\frac{d\Psi_f}{dz}\right)^2 = \frac{a^2}{12}\int_0^\infty dz \frac{1}{\Phi_f}\left(\frac{d\Phi_f}{dz}\right)^2 \quad (29)$$

This is equivalent to the following asymptotic approximation, proposed by Broseta et al.[19] and used by Semenov:[17]

$$F_{sf}(\infty)/a^{-2}kT = \frac{a^2}{12}\int_0^\infty dz \frac{1}{\Phi_f}\left(\frac{d\Phi_f}{dz}\right)^2 + \int_0^\infty dz \frac{\Phi_f}{N_f}\ln \Phi_f \quad (30)$$

When $N_f \gg N_g$, which is the case considered by GSA, eq 30 reduces to eq 29. Equations 22 and 29 give the result first obtained by Leibler and Ajdari:[13]

$$F_{sf}(\infty) \simeq \frac{kT}{\lambda a} \quad (31)$$

From the above consideration, we can now understand the origin of the attractive potential in $F_{pol}(H)$. We assume that eq 28 is valid even when the particle separation H becomes comparable to $2L$. The interaction potential can then be written as

$$F_{sf}(H)/a^{-2}kT = \frac{a^2}{12}\int_0^H dz \frac{1}{\Phi_f}\left(\frac{d\Phi_f}{dz}\right)^2 \quad (32)$$

Now, as the plates come close to each other, the segment density behaves as is shown in Figure 9: as the plates come close to each other, the tails of the brush overlap, and the minimum value of $\Phi_g(z)$ increases with a decrease of the separation H. According to eq 32, this change in $\Phi_g(z) = 1 - \Phi_f(z)$ decreases the attractive energy. In the limit of $H \to 2L$, $\Phi_f(z)$ has no dip at the center, and the attractive energy becomes zero. Hence, from eqs 20 and 31, it follows

$$\min F_{pol}(H) \simeq -\frac{kT}{\lambda a} \simeq -\frac{kT}{a^2}\left(\frac{\sigma a^2}{N_g}\right)^{1/3} \quad (33)$$

Thus, the maximum attractive energy is proportional to $\sigma^{1/3}$ in this approximation. Equation 33 is compared with the full mean field calculation in Figure 10. Although the agreement is not very good (we traced the main source of the error to the approximation of eq 28), eq 33 qualitatively explains the fact that the attractive energy increases with increasing graft density.

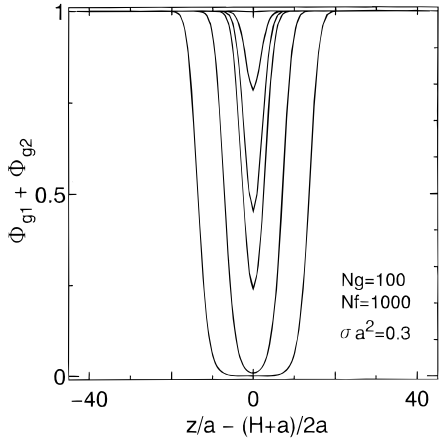

Figure 9. Segment density profile of $\Phi_g(z) = \Phi_{g_1}(z) + \Phi_{g_2}(z)$ of brushes ($N_g = 100$, $\sigma a^2 = 0.3$) in polymer matrix ($N_f = 1000$) for various sepaations H. The values of H/a are 60, 61, 63, 65, 74, and 87 from top to bottom.

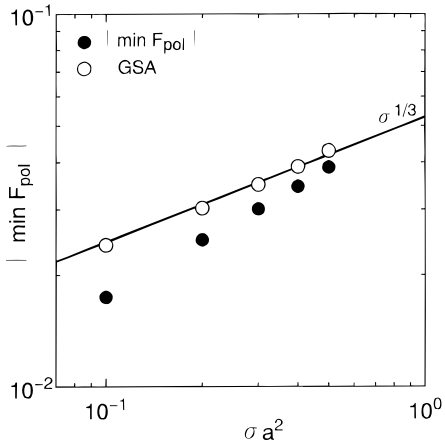

Figure 10. Comparison between mean field calculation and GSA for a dependence of the graft density σ on the interaction free energy $|\min F_{pol}|$. Here, $N_g = 100$ and $N_f = 1000$. The open circles denote the results of ground state approximation, and the filled circles denote that of the full mean field calculation.

It must be noted that eq 33 is valid in the brush regime, i.e., $\sigma a^2 \gtrsim N_g^{-1/2}$, only. In the mushroom regime, $\sigma a^2 \lesssim N_g^{-1/2}$, the grafted polymer is compressed as the plates come close to each other. This gives a positive (repulsive) contribution to the interaction energy. The energy of the compression per unit area is estimated by $kT\sigma(N_g^{1/2}a)^2/(N_g\sigma a^3)^2 = (kT/a^2)(N_g\sigma a^2)^{-1}$. On the other hand, the penetration depth λ is $N_g^{1/2}a$ in the mushroom regime, and the maximum attractive energy is $(kT/a^2)N_g^{-1/2}$, which is less than the compression energy. Therefore, in the mushroom regime, $F_{pol}(H)$ has only a repulsive part. This is, indeed, seen in Figure 4.

4. Discussion

In this paper, we have shown experimentally that there is an optimum graft density in dispersing polymer-grafted particles in a polymer matrix. We have shown theoretically that this is due to the interaction energy between the polymer brushes becoming attractive in the polymer matrix.

The origin of the attractive energy is, perhaps, the same as that predicted by Semenov[17] for the interaction between block copolymer micelles dispersed in ho-

mopolymer matrices. One can understand the origin of the attractive energy in the following simple way. In polymer melts, the brush and the matrix do not mix with each other, and there is a positive interfacial energy at the interface. If the brushes touch each other, then the interface between the brush and matrix disappears, and the free energy of the system decreases. This argument is crude, but it accounts for the fact that the attractive energy is strongest when the brushes touch each other.

We have shown that the attractive energy appears in the brush regime $\sigma a^2 \lesssim N_g^{-1/2}$. In the mushroom regime, $\sigma a^2 \lesssim N_g^{-1/2}$, $F_{pol}(H)$ has a repulsive part only. Thus, as a first approximation, we can estimate the optimum graft density by

$$\sigma_c \simeq N_g^{-1/2} a^{-2} \tag{34}$$

This estimation is crude: in general, the optimum graft density will depend not only on N_g but also on N_f since $F_{pol}(H)$ depends on N_f (see Figures 4 and 6). However, eq 34 will be a useful estimation for the optimum graft density for $N_g \simeq N_f$.

In this paper, we have assumed that both the graft polymer and the matrix polymer are monodisperse. Since the attraction takes place for nearly touching brushes, the effect of the molecular weight distribution is quite important. This effect will be discussed in future works.

Acknowledgment. The authors thank Prof. Kawakatsu for helpful discussion and the reviewer whose comments were useful in improving the original manuscript.

References and Notes

(1) Napper, D. H. *Polymeric Stabilization of Colloidal Dispersions*; Academic Press: New York, 1983.
(2) Israelachvili, J. N. *Intermolecular and Surface Forces*; Academic Press: London, 1985.
(3) de Gennes, P.-G. *Macromolecules* **1980**, *13*, 1069.
(4) Gast, A. P.; Leibler, L. *J. Chem. Phys.* **1985**, *89*, 3947; *Macromolecules* **1986**, *19*, 686.
(5) Aoki, Y. *Macromolecules* **1987**, *20*, 2208.
(6) Aoki, Y.; Nakayama, K. *Polym. J.* **1982**, *14*, 951.
(7) Aoki, Y.; Nakayama, K. *J. Soc. Rheol. Jpn.* **1981**, *9*, 39.
(8) Fleer, G. J.; Cohen Stuart, M. A.; Scheutjens, J. M. H. M.; Cosgrove, T.; Vincent, B. *Polymer at Interfaces*; Chapman and Hall: London, 1993; p 155.
(9) Wijmans, C. M.; Scheutjens, J. M. H. M.; Zhulina, E. B. *Macromolecules* **1992**, *25*, 2657.
(10) Wijmans, C. M.; Zhulina, E. B.; Fleer, G. J. *Macromolecules* **1994**, *27*, 3238.
(11) Aubouy, M.; Brochard, F.; Raphael, E. *Macromolecules* **1993**, *26*, 5885.
(12) Aubouy, M.; Fredrickson, G. H.; Pincus, P.; Raphael, E. *Macromolecules* **1995**, *28*, 2979.
(13) Leibler, L.; Ajdari, A. In *Ordering in Macromolecular Systems*; Teramoto, A., Kobayashi, M., Norisue, T., Eds.; Springer: New York, 1994; p 301.
(14) Semenov, A. N. *Sov. Phys. J.E.T.P.* **1985**, *61*, 733. Milner, S. T.; Witten, T. A.; Cates, M. E. *Macromolecules* **1988**, *21*, 2610. Zhulina, E. B.; Priamitsyn, V. A.; Borisov, O. V. *Polym. Sci. USSR* **1989**, *31*, 205.
(15) Fredrickson, G. In *Physics of Polymer Surfaces and Interfaces*; Sanchesz, I. C., Ed.; Butterworth-Heinemann: Boston, MA, 1992; p 1.
(16) Semenov, A. N. *Macromolecules* **1992**, *25*, 4967.
(17) Semenov, A. N. *Macromolecules* **1993**, *26*, 2273.
(18) Matsen, M. W. *Macromolecules* **1995**, *28*, 5765.
(19) Broseta, D.; Fredrickson, G. H.; Helfand, E.; Leibler, L. *Macromolecules* **1990**, *23*, 132.
(20) Kato, K. J. *Electron Microsc.* **1965**, *14*, 220.
(21) Derjagin, B. V. *Kolloid Z.* **1934**, *69*, 155.

MA960365X